

A test on external Compton models for γ -ray active galactic nucleiZhonghui Fan^{1,2}, Xinwu Cao¹, Minfeng Gu¹**ABSTRACT**

There is clear evidence that the γ -ray emission from active galactic nuclei (AGNs) is attributed to the inverse Compton scatterings in the relativistic blobs near the massive black holes. If the soft seed photons are from the regions outside the blobs, a linear relation between $(\nu F_{\nu,\gamma}/\nu F_{\nu,\text{syn}} u^*)^{1/(1+\alpha)}$ and Doppler factor δ is expected, where $\nu F_{\nu,\gamma}$ and $\nu F_{\nu,\text{syn}}$ are monochromatic γ -ray and synchrotron fluxes, respectively, and u^* is the energy density of soft seed photons (Dermer, Sturmer & Schlickeiser 1997). We estimate the soft photon energy density in the relativistic blobs contributed by the broad line region (BLRs) in these γ -ray AGNs using their broad-line emission data. The Doppler factors δ are derived from their radio core and X-ray emission data, based on the assumption that the X-ray emission is produced through synchrotron self-Compton (SSC) scatterings. We find two nearly linear correlations: $(\nu F_{\nu,\gamma}/\nu F_{\text{opt}} u^*)^{1/(1+\alpha)} \propto \delta^{1.09}$, and $(\nu F_{\nu,\gamma}/\nu F_{\text{IR}} u^*)^{1/(1+\alpha)} \propto \delta^{1.20}$, which are roughly consistent with the linear correlation predicted by the theoretical model for external Compton scatterings. Our results imply that the soft seed photons are dominantly from the BLRs in these γ -ray AGNs.

Subject headings: galaxies: active — gamma rays: theory — radiation mechanisms: nonthermal — black hole physics

1. Introduction

All γ -ray AGNs are identified as flat-spectrum radio sources. The third catalog of high-energy γ -ray sources detected by the Energetic Gamma Ray Experiment Telescope

¹Shanghai Astronomical Observatory, Chinese Academy of Sciences, Shanghai 200030, China
E-mail: fanzh@shao.ac.cn; cxw@shao.ac.cn; gumf@shao.ac.cn

²Graduate School of the Chinese Academy of Sciences, BeiJing 100039, China

(EGRET) on the Compton Gamma Ray Observatory (CGRO) includes 66 high-confidence identifications of blazars and 27 lower confidence potential blazar identifications (Hartman et al. 1999). This provides a good sample for the explorations on the radiative mechanisms of γ -rays from AGNs. The violent variations in very short time-scales imply that the γ -ray emission is closely related with the relativistic jets in blazars. There are two kinds of models, namely, leptonic models and hadronic models, proposed for γ -ray emission in blazars (see Mukherjee 2001 for a review). According to the different origins of the soft photons, the leptonic models can be classified as two groups: synchrotron self-Compton (SSC) models and external radiation Compton (EC) models (see Sikora & Madejski 2001 for a review).

In the frame of SSC models, the synchrotron photons are both produced and Compton up-scattered by the same population of relativistic electrons in the jets of γ -ray blazars. The synchrotron radiation is responsible for the low energy component in radio bands, and the synchrotron photons are Compton up-scattered to γ -ray photons by the same population of relativistic electrons in the jets (Morganti, Ulrich & Tadhunter 1992). However, SSC models meet difficulties with the observed rapidly variable fluxes in MeV-GeV for some blazars. It has been realized that the processes other than SSC may occur at least in some γ -ray blazars. One possibility is soft seed photons being from the external radiation fields outside the jets, namely, EC models. The origins of soft seed photons may include the cosmic microwave background radiation, the radiation of the accretion disk (including photons from the disk scattered by surrounding gas and dust), infrared emission from the dust or/and a putative molecular torus, and broad line region (BLRs), etc (Dermer & Schlickeiser 2002). Recently, Sikora et al. (2002) proposed that the external radiation is from the BLRs for GeV γ -ray blazars with flat γ -ray spectra, while the near-IR radiation from the hot dust is responsible for MeV γ -ray blazars with steep γ -ray spectra. In their model, the electrons are assumed to be accelerated via a two-step process and their injection function takes the form of a double power law with a break at the energy that divides the regimes for two different electron acceleration mechanisms.

The relations between γ -ray emission and emission in different wavebands (such as optical, infrared and radio bands) may provide clues on the radiative mechanism for γ -ray emission (e.g., Zhou et al. 1997, Fan et al. 1998, Dondi & Ghisellini 1995, Zhang, Cheng & Fan 2001, Yang & Fan 2005). However, all these correlation analysis cannot distinguish between the EC and SSC models for γ -ray emission. Dermer, Sturmer & Schlickeiser (1997) investigated the γ -ray radiation from a homogeneous spherical blob relativistically moving away from the central black hole. Their calculations predicted a linear relation between $(\nu F_{\nu,\gamma}/\nu F_{\nu,\text{syn}} u^*)^{1/(1+\alpha)}$ and Doppler factor δ , if the EC model is responsible for the γ -ray radiation. Here $\nu F_{\nu,\gamma}$ and $\nu F_{\nu,\text{syn}}$ are monochromatic γ -ray and synchrotron fluxes, respectively, u^* is the energy density of soft seed photons, and α is the photon energy

spectral index of γ -rays. For the SSC model, their calculations showed that $\nu F_{\nu,\gamma}/\nu F_{\nu,\text{syn}}u^*$ is independence of δ . Huang, Jiang & Cao (1999) analyzed the correlations between the ratio of γ -ray flux to the fluxes in different wavebands and δ for a sample of EGRET AGNs. They found significant correlations between $F_\gamma/\nu F_{\text{opt}}$ and δ , $F_\gamma/\nu F_{\text{IR}}$ and δ . Their results suggested that the EC model is responsible for γ -ray emission, though the origin of the soft seed photons is still unclear.

Several different approaches are proposed to estimate the Doppler factors δ of the jets in AGNs. Ghisellini et al. (1993) derived the synchrotron self-Compton Doppler factor δ_{SSC} of the jets in AGNs from the VLBI core sizes and fluxes, and X-ray fluxes, on the assumption of the X-ray emission being produced by the SSC processes in the jets. Güijosa & Daly (1996) assumed energy equipartition between the particles and the magnetic fields in the jet components, and derived the equipartition Doppler factor δ_{eq} . The variability Doppler factor δ_{var} is derived on the assumption that the associated variability brightness temperature of total radio flux density flares are caused by the relativistic jets (Lähteenmäki & Valtaoja 1999).

In this paper, we use the multi-waveband data of γ -ray AGNs to explore the radiative mechanism of γ -rays for these AGNs. The Doppler factors δ are derived from VLBI and X-ray data by using Ghisellini et al.’s approach. The cosmology with $H_0 = 70 \text{ km s}^{-1} \text{ Mpc}^{-1}$, $\Omega_{\text{M}} = 0.3$, and $\Omega_{\Lambda} = 0.7$ have been adopted throughout the paper.

2. Model

2.1. External Compton model

In this paper, we mainly follow the model proposed by Dermer, Sturmer & Schlickeiser (1997). We briefly summarize their model here (see Dermer, Sturmer & Schlickeiser 1997 for details). Assuming that the seed photons are produced externally to the jet, one can predict a correlation between the Doppler factor δ and the ratio of the γ -ray flux to the synchrotron radiation flux, $\nu F_{\nu,\gamma}/\nu F_{\nu,\text{syn}}$, as shown by Eq. (27) in Dermer, Sturmer & Schlickeiser (1997):

$$\rho_{\text{C/syn}} = \frac{\nu F_{\nu,\gamma}}{\nu F_{\nu,\text{syn}}} \approx \left(\frac{\epsilon_s \bar{\epsilon}^*}{\epsilon_C \epsilon_H} \right)^{\alpha-1} \frac{u_i^*}{u_H} \delta^{1+\alpha} \quad (1)$$

where α is the photon energy spectral index of γ -rays; u_i^* and u_H denote the energy density of monochromatic photons in the external target radiation field and the blob’s magnetic field ($u_H = B^2/8\pi$, where the magnetic field strength is $B \equiv 4.414 \times 10^{13} \epsilon_H$), respectively; $\bar{\epsilon}^*$ is monochromatic photon energy in the stationary frame, ϵ_s and ϵ_C are the synchrotron photon

energy and inverse Compton scattering photon energy in blob frame, respectively. Assuming that

$$(\epsilon_s \bar{\epsilon}^*) / (\epsilon_C \epsilon_H) \simeq 1 \quad (2)$$

(Dermer, Sturmer & Schlickeiser 1997), Eq. (1) then becomes

$$\rho_{C/\text{syn}} \approx \frac{u_i^*}{u_H} \delta^{1+\alpha}. \quad (3)$$

For the homogeneous SSC model, the flux ratio of the SSC spectral power flux to the synchrotron spectral power flux $\rho_{\text{SSC}/\text{syn}}$ is independence of Doppler factor δ (see Eq. (28) in Dermer, Sturmer & Schlickeiser 1997):

$$\rho_{\text{SSC}/\text{syn}} = \frac{\nu F_{\nu,\gamma}}{\nu F_{\nu,\text{syn}}} = \frac{2}{3} (\sigma_T n_{eo} r_b) \left(\frac{\epsilon_s}{\epsilon_C} \right)^{\alpha-1} \ln \bar{\Sigma}_C(\epsilon_C) \propto n_{eo}, \quad (4)$$

where σ_T is the Thomson cross section, r_b is the radius of the blob, n_{eo} is the normalization factor of the number density of nonthermal electrons, and $\bar{\Sigma}_C$ is the transformed Compton-synchrotron logarithm (see Eq. (25) in Dermer, Sturmer & Schlickeiser 1997)

$$\bar{\Sigma}_C(\epsilon_C) \equiv \frac{\min\{\delta/[\epsilon_C(1+z)], \gamma_2^2 \epsilon_H, \epsilon_C(1+z)/(\delta\gamma_1^2)\}}{\max[\gamma_1^2 \epsilon_H, \epsilon_C(1+z)/(\delta\gamma_2^2)]}, \quad (5)$$

where γ_1 and γ_2 are the lower limit and upper limit of electronic Lorentz factors in the blob.

2.2. Soft seed photon energy density

In the EC models, the energy density of seed photon fields in a blob may be the summation of the cosmic microwave background radiation, the radiation of the accretion disk (including photons from the disk scattered by surrounding gas and dust), infrared emission from the dust and/or a putative molecular torus, and the BLRs, etc.. In this work, we only focus on the soft seed photons contributed by the broad line emission.

In principle, all broad emission line fluxes are needed to calculate the total soft seed photon energy in the blobs contributed by different broad emission lines. Usually, the fluxes of only one or several broad emission lines are available for most sources in our sample due to the restriction of redshift. We use the line ratios presented by Francis et al. (1991), in which the relative strength of Ly α is taken as 100, to convert the flux of available lines into the flux of H β line. Celotti, Padovani & Ghisellini (1997) added the contribution from the flux of H α $F_{\text{H}\alpha}$, with a value of 77. This gives a total relative flux $\langle F_{\text{BLR}} \rangle = 555.77$ (narrow lines are not included). Due to the significant beaming effect in the optical continuum emission,

we use the relation between the BLR size and H_β luminosity (Wu et al. 2004) to estimate the BLR radius. We re-fit their data and obtain the correlation between L_{H_β} and R_{BLR} :

$$\log R_{\text{BLR}} (\text{light} - \text{days}) = (1.323 \pm 0.086) + (0.667 \pm 0.101) \log (L_{H_\beta}/10^{42} \text{ ergs s}^{-1}), \quad (6)$$

for the present cosmology adopted in this paper. We calculate the total photon energy density of the soft seed photons in the blob from BLRs as (Fan & Cao 2004)

$$u_{\text{BLR}}^* = \sum u_i^* \approx \frac{555.77}{22} \times u_{H_\beta}^*. \quad (7)$$

The energy density $u_{H_\beta}^*$ of H_β emission line in the blob is given by

$$u_{H_\beta}^* = \frac{1}{c} \left(\frac{d_L}{R_{\text{BLR}}} \right)^2 F_{H_\beta}, \quad (8)$$

where d_L is the luminosity distance, F_{H_β} is the flux of H_β emission line, and Eq. (8) is valid for the blob near the central black hole.

2.3. The Doppler factor

In this work, the Doppler factors δ are derived from the VLBI radio core and X-ray emission data based on the assumption that the X-ray emission is produced through synchrotron self-Compton (SSC) processes. In the case of a moving sphere ($p = 3 + \alpha$) (see Ghisellini et al. 1993 for details), δ of the blob can be given as:

$$\delta = f(\alpha) F_c \left[\frac{\ln(\nu_b/\nu_s)}{F_X \theta_d^{6+4\alpha} \nu_x^\alpha \nu_s^{5+3\alpha}} \right]^{1/(4+2\alpha)} (1+z), \quad (9)$$

where F_c is the VLBI core radio flux density (in Jy) observed at ν_s (GHz), θ_d is the VLBI core size (in mas), F_X is the X-ray flux density (in Jy) observed at ν_x (keV), ν_b is the synchrotron high frequency cutoff (assumed to be 10^{14} Hz), and the function $f(\alpha) = 0.08\alpha + 0.14$ (here $\alpha = 0.75$ is assumed).

3. The Sample

We search the literature and collect all available data of γ -ray AGNs in EGRET catalog III. This leads to 40 sources, of which 34 sources are the high-confidence identification blazars and 6 sources are the lower confidence potential blazar identifications listed in Hartman et al. (1999).

Table 1 lists the VLBI and X-ray observations: (1) IAU name; (2) confidence (A is high-confidence identifications of blazars, a is lower confidence identifications of potential blazars); (3) type classification of the source (BL=BL Lac object, Q= quasar); (4) redshift; (5) VLBI core size θ_d in mas; (6) core radio flux density F_c at frequency ν_s ; (7) observation frequency ν_s in GHz; (8) reference for the VLBI data; (9) 1 keV X-ray flux density F_X in μJy ; (10) reference for the X-ray flux; (11) calculated Doppler factor δ . The classification of sources is according to the 11th edition catalogue of quasars and active nuclei (Véron-Cetty & Véron 2003). For those sources which have multi-frequency VLBI observations, the VLBI data at the highest frequency are chosen.

Table 2 lists the multiwavelength flux data and the flux density of H_β emission line: (1) IAU name; (2) the photon energy spectral index of γ -rays; (3) γ -ray flux above 100 MeV, F_γ , in unit of 10^{-8} photon $\text{cm}^{-2} \text{s}^{-1}$; (4) V-band optical flux density F_{opt} in mJy; (5) reference for the optical flux density; (6) near infrared flux density F_{IR} at $2.2 \mu\text{m}$ in mJy; (7) reference for the infrared flux density at $2.2 \mu\text{m}$; (8) flux density at 5 GHz; (9) reference for the flux density at 5 GHz; (10) flux density of H_β emission line, in unit of 10^{-15} ergs $\text{cm}^{-2} \text{s}^{-1}$; (11) reference for the flux density of H_β ; (12) the total soft photon energy density u_{BLR}^* in the blob from BLRs, in units of ergs cm^{-3} . The maximal values of the infrared flux data are chosen from the literature when more than one data are available. For six sources, we adopt the infrared flux from 2MASS archive. For the sources without flux density of H_β emission line, we convert the flux density of other emission lines into the flux density of H_β emission line, as described in Sect. 2.2, which is used to estimate the BLR size.

4. Results

We use the relation between BLR size and H_β line luminosity to calculate the BLR radius. The total photon energy in the blob of the soft seed photons from BLRs are then estimated from Eq. (6). The Doppler factors δ are derived from radio core and X-ray emission data, as described in § 2.3. Assuming that the seed photons are from BLRs, we investigate the correlation between Doppler factor δ and the ratio of the γ -ray flux to the synchrotron radiation flux. All the observational data and results are listed in Tables 1 – 4. The derived synchrotron self-Compton Doppler factors δ are listed in Column (11) of Table 1. The derived total photon energy densities of the soft seed photons in the blob’s frame from BLRs u_{BLR}^* are listed in Column (12) of Table 2.

The γ -ray emission from these sources is violently variable. In our analysis, we use the maximal integrated γ -ray fluxes F_γ (> 100 MeV) for each source (Hartman et al. 1999). The monochromatic flux at 100 MeV, 1 GeV and 20 GeV (i.e. νF_ν) are estimated from

these maximal integrated γ -ray fluxes by assuming that the SED of γ -ray is characterized as a power law $F_\nu \propto \nu^{-\alpha}$ (Hartman et al. 1999).

The results of our correlation analysis are shown in Tables 3 and 4. In both Tables, Columns (1) and (2), list two variables used in analysis. Column (3) lists the number of sources. Columns (4) and (6) list the intercept and the slope of the fitted line using OLS bisector method (Isobe et al. 1990), respectively. Columns (5) and (7) are the standard deviations of intercept and slope, respectively. Column (8) lists the pearson correlation coefficient. Column (9) lists the chance probability.

The relations of the Doppler factor δ versus the flux ratio $(\nu F_{\nu,\gamma}/\nu F_{\nu,\text{syn}} u_{\text{BLR}}^*)^{1/(1+\alpha)}$ are plotted in Fig. 1. The top, middle, and bottom panels in Fig. 1 are the cases for F_γ at 100 MeV, 1 GeV and 20 GeV, respectively. While all left panels are for F_{syn} at 5500 Å, all right panels are for F_{syn} at 2.2 μm . In Table 3, it can be seen that there are significant correlations between δ and $(\nu F_{\nu,\gamma}/\nu F_{\text{opt}} u_{\text{BLR}}^*)^{1/(1+\alpha)}$, δ and $(\nu F_{\nu,\gamma}/\nu F_{\text{IR}} u_{\text{BLR}}^*)^{1/(1+\alpha)}$. Using OLS bisector method, we obtain:

$$\log \left[\frac{\nu F_{100\text{MeV}}}{(\nu F_{\text{opt}}) u_{\text{BLR}}^*} \right]^{\frac{1}{1+\alpha}} = (0.481 \pm 0.105) + (1.089 \pm 0.092) \log \delta, \quad (10)$$

and

$$\log \left[\frac{\nu F_{100\text{MeV}}}{(\nu F_{\text{IR}}) u_{\text{BLR}}^*} \right]^{\frac{1}{1+\alpha}} = (0.253 \pm 0.128) + (1.203 \pm 0.104) \log \delta. \quad (11)$$

The correlations are at a confidence level of 99.93 per cent for optical flux at 5500 Å, and at a confidence level of 99.55 per cent for infrared flux at 2.2 μm , in the case of γ -ray monochromatic flux at 100 MeV. When BL Lac objects are excluded, the similar correlations are still present (see Table 3). The results are similar for the cases of γ -ray at 1 GeV. For radio flux at 5 GHz, we have not found any significant correlations between $(\nu F_{\nu,\gamma}/\nu F_{5\text{GHz}} u_{\text{BLR}}^*)^{1/(1+\alpha)}$ and δ . For the average integrated γ -ray flux, we also find the similar results, but the correlations are slightly weaker compared with those for the maximum integrated γ -ray flux.

In Fig. 2, we plot the relations between $F_\gamma/\nu F_{\nu,\text{syn}}$ and δ for different wavebands (optical, IR, and radio), without considering the soft photon energy u^* , which are similar to those as done by Huang, Jiang & Cao (1999) (They used $(\nu F_\nu)_\gamma$ to represent the integrated γ -ray flux, instead of the integrated γ -ray flux F_γ used in this work). We have not found any correlations between $F_\gamma/\nu F_{\nu,\text{syn}}$ and δ for each waveband (see Table 4 for details), which are different from those given by Huang, Jiang & Cao (1999).

5. Discussion

In most previous works, the size of the BLR is usually estimated from the optical or UV continuum luminosity (e.g., Kaspi et al. 2000, Mclure & Jarvis 2002, Vestergaard 2002). However, for γ -ray blazars, the observed optical/UV continuum emission may be dominantly from the relativistic jets, which is strongly beamed to us. In this work, we estimate the size of the BLR from H_β luminosity instead of the optical or UV continuum luminosity, and then the soft photon energy density in the blob.

We have found significant correlations $(\nu F_{\nu,\gamma}/\nu F_{\text{opt}} u_{\text{BLR}}^*)^{1/(1+\alpha)} - \delta$ and $(\nu F_{\nu,\gamma}/\nu F_{\text{IR}} u_{\text{BLR}}^*)^{1/(1+\alpha)} - \delta$, of which the slopes are close to unity. These are consistent with the prediction of the EC model (see Eq. 3). For the SSC model, the ratio of $\nu F_{\nu,\gamma}/\nu F_{\nu,\text{syn}}$ should be independent of δ (see Eq. 4). Our results imply that the γ -ray emission may be dominated by EC processes, rather than SSC processes, at least for the γ -ray blazars in this sample. On the origins of the external soft seed photons, Sikora, Begelman & Rees (1994) proposed that the dominant contribution to the energy density, as measured in the comoving frame of the radiating plasma, comes from scattered or reprocessed portions of the central source radiation, rather than from the direct radiation of the central source. For an accretion disk, if a blob is sufficiently far from the central engine of the AGN so that the accretion disk can be approximated as a point source of photons, its photon energy density (in the comoving frame) is $u'_D \approx L_D/(4\pi z^2 c \Gamma^2)$, where L_D is the accretion disk luminosity, z is the height of the blob above the accretion disk, and Γ is the Lorentz factor of the blob. Because of the blob leaves from the disk with high velocity, soft photons from the disk are strongly redshifted. For BLR, the reprocessed radiation is nearly isotropic in the rest-frame of the central engine, it will be strongly blue-shifted in the rest-frame of the relativistically moving blob. Thus, the ratio of the soft photon energy density measured in the rest frame of the blob, $u_{\text{EC}}^{\text{BLR}}/u'_D \sim a_{\text{BLR}}(z/\langle r \rangle_{\text{BLR}})^2 \Gamma^4 \gg 1$, where the fraction of the radiation rescattered into the jet trajectory $a_{\text{BLR}} \sim 0.1$, and $\langle r \rangle_{\text{BLR}}$ is the average distance of the BLR from the central black hole (Böttcher 1999). For torus, the typical thickness of the dust torus H/R is around unity (e.g., Cao 2005), so that only a small fraction of the photons from the disk are scattered by the torus. The size of the torus is much larger than that of the BLR. So, the soft photon energy density contributed by the torus can be neglected compared with that from the BLR. Although only the soft seed photons from the BLRs are considered in this work, the results are in good agreement with the model predictions, which implies that the soft photons are dominated from the BLRs. Huang, Jiang & Cao (1999) found significant correlations between $F_\gamma/\nu F_{\nu,\text{syn}}$ and δ for IR and optical bands, while no correlation is present for our sample. There may be two reasons, (1) the present sample consisting of 40 sources, which is larger than theirs, (2) we adopt VLBI core sizes measured at higher frequencies for some sources, and the derived Doppler factors are therefore more reliable.

We note that the results of Huang, Jiang & Cao (1999) implied that the equipartition parameter $\kappa_{\text{eq}} \equiv u_i^*/u_H$ remains constant between different sources. Our results imply that the equipartition parameter κ_{eq} may not be constant. This is may be one of reasons of the lack of correlation in Fig. 2.

We note that Eq. (3) can be re-expressed as

$$\log[\nu F_\gamma/(\nu F_{\text{syn}}u_{\text{BLR}})]^{1/(1+\alpha)} = A_1 + A_2 \log(B) + \log(\delta), \quad (12)$$

which can then be used to constrain the magnetic field strength B by using Eq. (10) & (11). We can find $B \sim 1.7 - 2.8$ Gauss. Assuming $(\epsilon_s \bar{\epsilon}^*)/(\epsilon_C \epsilon_H) = 1$, $\bar{\epsilon}^*$ is $H\beta$ emission line photon energy at 4861 Å in the stationary frame, the synchrotron photon energy ϵ_s is in optical-Infrared region, γ -ray photon energy ϵ_C is 100 MeV, we find that the magnetic field strength B in the blob frame is about 2 Gauss. We can see that the magnetic field strength derived from equations (10) & (11) is agreement with the model predictions. Moreover, these values of the magnetic field strength are consistent with other researches (e.g., Maraschi & Tavecchio 2003). From $(\epsilon_s \bar{\epsilon}^*)/(\epsilon_C \epsilon_H) = 1$, we also can constrain the spectral region, in which the synchrotron emission are radiated by the electron population, responsible for γ -ray emission through inverse Compton process. we find that the synchrotron photon frequency corresponding to 100 MeV γ -ray photons are in optical-Infrared region. This is in good agreement with the significant correlations we found. However, for 5 GHz radio photons, the corresponding photon energies via inverse Compton scattering may be much lower than 100 MeV. In addition, the total 5 GHz radio flux of these γ -ray sources are dominated by the radio core emission, which is usually from optically thick region. These can explain why there is no significant correlations between $(\nu F_{\nu,\gamma}/\nu F_{5\text{GHz}}u_{\text{BLR}}^*)^{1/(1+\alpha)}$ and δ .

In this work, we use SSC model to estimate δ assuming X-ray is due to the SSC process. Our results show that γ -ray may probably be produced by the EC process. Fitting the simultaneous broadband spectrum of the FSRQ 3C279, Hartman et al. (2001) found that the SSC model can fit the observed X-ray data very well, while the EC model can fit to the γ -ray data successfully. For PKS 0528+134, a similar conclusion was drawn by Mukherjee et al. (1999).The BLR photons are mainly in optical/UV bands, and they are strongly blueshifted to higher frequencies measured in the blob frame with a factor of $\sim \Gamma$. So the observed energy of the BLR photons scattered by the relativistic electrons in the blob should at least in the range of $\sim \Gamma^2 \gamma_{e,\text{min}}^2 \epsilon_{\text{BLR}}^*$, which should be much higher than 1 keV, for typical values $\Gamma \sim 10$, the lower limit of electronic Lorentz factors $\gamma_{e,\text{min}} \sim 100$ adopted (e.g., Celotti & Fabian 1993). Even for the photons from the disk or torus, the energy of the scattered photons by the blobs is also higher than 1 keV. So the X-ray emission at 1 keV should be produced by SSC process.

No obvious statistic difference is found between BL Lac objects and quasars in this

sample (see Table 3), though the SSC model is supposed to be responsible for γ -rays from BL Lac objects (e.g. Dondi & Ghisellini 1995), and the γ -ray variability properties of flat-spectrum quasars are different from those of BL Lac objects (Vercellone et al. 2004). There are only 6 γ -ray BL Lac objects in our sample, and the remainder (10 BL Lacs) in the EGRET AGNs catalogue are not included in this sample, because of the lack of broad-line emission data for those BL Lac objects. All the BL Lac objects in the present sample have relatively stronger broad lines among the whole catalog of BL Lac objects. The BL Lac objects included in this sample are more similar to quasars. These BL Lac objects are somewhat special, which may be in the stage of the transition from quasars to BL Lac objects (e.g. Cao 2003). For those 10 γ -ray BL Lac objects without broad emission lines, the SSC mechanism may be important for their γ -ray emission, which is beyond the scope of this paper.

We are thankful to the referee for insightful comments and constructive suggestions that helped to improve this paper. This work is supported by the National Science Foundation of China (grants 10325314, 10333020, and 10543002). This research has made use of the NASA/IPAC Extragalactic Database (NED), which is operated by the Jet Propulsion Laboratory, California Institute of Technology, under contract with the National Aeronautics and Space Administration. This publication makes use of data products from the Two Micron All Sky Survey, which is a joint project of the University of Massachusetts and the Infrared Processing and Analysis Center/California Institute of Technology, funded by the National Aeronautics and Space Administration and the National Science Foundation.

REFERENCES

- Baldwin, J. A., Wampler, E. J., & Gaskell, C. M. 1989, *ApJ*, 338, 630
- Barkhouse, W. A., & Hall, P. B. 2001, *AJ*, 121, 2843
- Bloom, S. D. et al. 1994, *AJ*, 108, 398
- Böttcher, M. 2000, *AIPC*, 515, 31
- Celotti, A., & Fabian, A. C. 1993, *MNRAS*, 264, 228
- Celotti, A., Padovani, P., & Ghisellini, G. 1997, *MNRAS*, 286, 415
- Cao, X. 2003, *ApJ*, 599, 147
- Cao, X. 2005, *ApJ*, 619, 86

- Chapuis, C. et al. 1999, ASPC, 159, 97
- Cohen, R. D., Smith, H. E., Junkkarinen, V. T., & Burbidge, E. M. 1987, ApJ, 318, 577
- Comastri, A., Fossati, G., Ghisellini, G., & Molendi, S. 1997, ApJ, 480, 534
- Dermer, C. D., Sturmer, S. J., Schlickeiser, R. 1997, ApJS, 109, 103
- Dermer, C. D., & Schlickeiser, R. 2002, ApJ, 575, 667
- Dondi, L., & Ghisellini, G. 1995, MNRAS, 273, 583
- Falomo, R., Bersanelli, M., Bouchet, P., & Tanzi, E. G. 1993, AJ, 106, 11
- Fan, J. H. et al. 1998, A&A, 338, 27
- Fan, Z. H., & Cao, X. W. 2004, ApJ, 602, 103
- Fey, A. L., & Charlot, P. 2000, ApJS, 128, 17
- Fomalont, E. B., & Frey, S. et al. 2000, ApJS, 131, 95
- Francis, P. J., Hewett, P. C., Foltz, C. B., Chaffee, F. H., Weymann, R. J., Morris, S. L. 1991, ApJ, 373, 465
- Gear, W. K. et al. 1985, ApJ, 291, 511
- Ghisellini, G., Padovani, P., Celotti, A., & Maraschi, L. 1993, ApJ, 407, 65
- Gu, M. F, Cao, X., & Jiang, D. R. 2001, MNRAS, 327, 1111
- Güijosa, A., & Daly, R. A. 1996, ApJ, 461, 600
- Hartman, R. C. et al. 1999, ApJS, 123, 79
- Hartman, R. C. et al. 1999, ApJ, 553, 683
- Huang, L. H, Jiang, D. R., & Cao, X. W. 1999, A&A, 341, 74
- Hunstead, R. W., Murdoch, H. S., & Shobbrook, R. R. 1978, MNRAS, 185, 149
- Isobe, T., Feigelson, E. D., Akritas, M. and Babu, G. J. 1990, ApJ, 364, 104
- Jackson, N., & Browne, W. A. 1991, MNRAS, 250, 414
- Jorstad, S. G. et al. 2001, ApJS, 134, 181

- Junkkarinen, V. 1984, *PASP*, 96, 539
- Kaspi, S., et al. 2000, *ApJ*, 533, 631
- Koratkar et al. 1998, *ApJ*, 492, 173
- Küehr, H., Witzel, A.; Pauliny-Toth, I. I. K., & Nauber, U. 1981, *A&AS*, 45, 367
- Lähteenmäki, A., & Valtaoja, E. 1999, *ApJ*, 521, 493
- Lawrence, C. R. et al. 1996, *ApJ*, 107, 541
- Lister, M. L. 2001, *ApJ*, 562, 208
- Maraschi, L. & Tavecchio, F. 2003, *ApJ*, 593, 667
- Marcha, M. J. M., Browne, I. W. A., Impey, C. D., & Smith, P. S. 1996, *MNRAS*, 281, 425
- Marshall, H. L. et al. 2005, *ApJS*, 156, 13
- McLure, R. J., & Jarvis, M. J. 2002, *MNRAS*, 337, 109
- Mead, A. R. G. et al. 1990, *A&AS*, 83, 183
- Morganti, R., Ulrich, M.-H., & Tadhunter, C. N. 1992, *MNRAS*, 254, 546
- Mukherjee, R. et al. 1999, *ApJ*, 527, 132
- Mukherjee, R. 2001, in *AIP Conf. Proc. 558, High Energy Gamma-Ray Astronomy*, ed. by F. A. Aharonian & H. J. Völk (New York: AIP), 324
- Petry, D. et al. 2000, *ApJ*, 536, 742
- Sambruna, R. M., Maraschi, L., & Urry, C. M. 1996, *ApJ*, 463, 444
- Scarpa, R., & Falomo, R. 1997, *A&A*, 325, 109
- Shen, Z. Q. et al. 1998, *AJ*, 115, 1357
- Siebert, J. et al. 1998, *MNRAS*, 301, 261
- Sikora, M., Begelman, M. C. & Rees, M. 1994, *ApJ*, 421, 153
- Sikora, M., & Madejski, G. 2001, in *AIP Conf. Proc. 558, High Energy Gamma-Ray Astronomy*, ed. by F. A. Aharonian & H. J. Völk (New York: AIP), 275
- Sikora, M., Blazejowski, M., Moderski, R., & Madejski, G. M. 2002, *ApJ*, 577, 78

- Stickel, M., Fried, J. W., & Kühr, H. 1989, *A&AS*, 80, 103
- Stickel, M., Kühr, H., & Fried, J. W. 1993, *A&AS*, 97, 483
- Stockton, A., & Mackenty, J. W. 1987, *ApJ*, 316, 584
- Vercellone, S., Soldi, S., Chen, A. W. & Tavani, M. 2004, *MNRAS*, 353, 890
- Vermeulen, R. C. et al. 1995, *ApJ*, 452, 5
- Véron-Cetty, M. -P., & Véron, P. 2003, *A&A*, 412, 399
- Vestergaard, M. 2002, *ApJ*, 571, 733
- Wampler, E. J., Gaskell, C. M., Burke, W. L. 1984, *ApJ*, 276, 403
- Wilkes, B. J. 1986, *MNRAS*, 218, 331
- Wilkes, Belinda J. et al. 1994, *ApJS*, 92, 53
- Wills, B. J. et al. 1983, *ApJ*, 274, 62
- Wills, B. J., et al. 1995, *ApJ*, 447, 139
- Wu, X. B., et al. 2004, *A&A*, 424, 793
- Xie, G. Z., Zhang, X., Bai, J. M., & Xie, Z. H. 1998, *ApJ*, 508, 180
- Yang, J. H., & Fan, J. H. 2005, *ChJAA*, 5, 229
- Zhang, L., Cheng, K. S., & Fan, J. H. 2001, *PASJ*, 53, 207
- Zhou, Y., Y. et al. 1997, *ApJ*, 484, 47

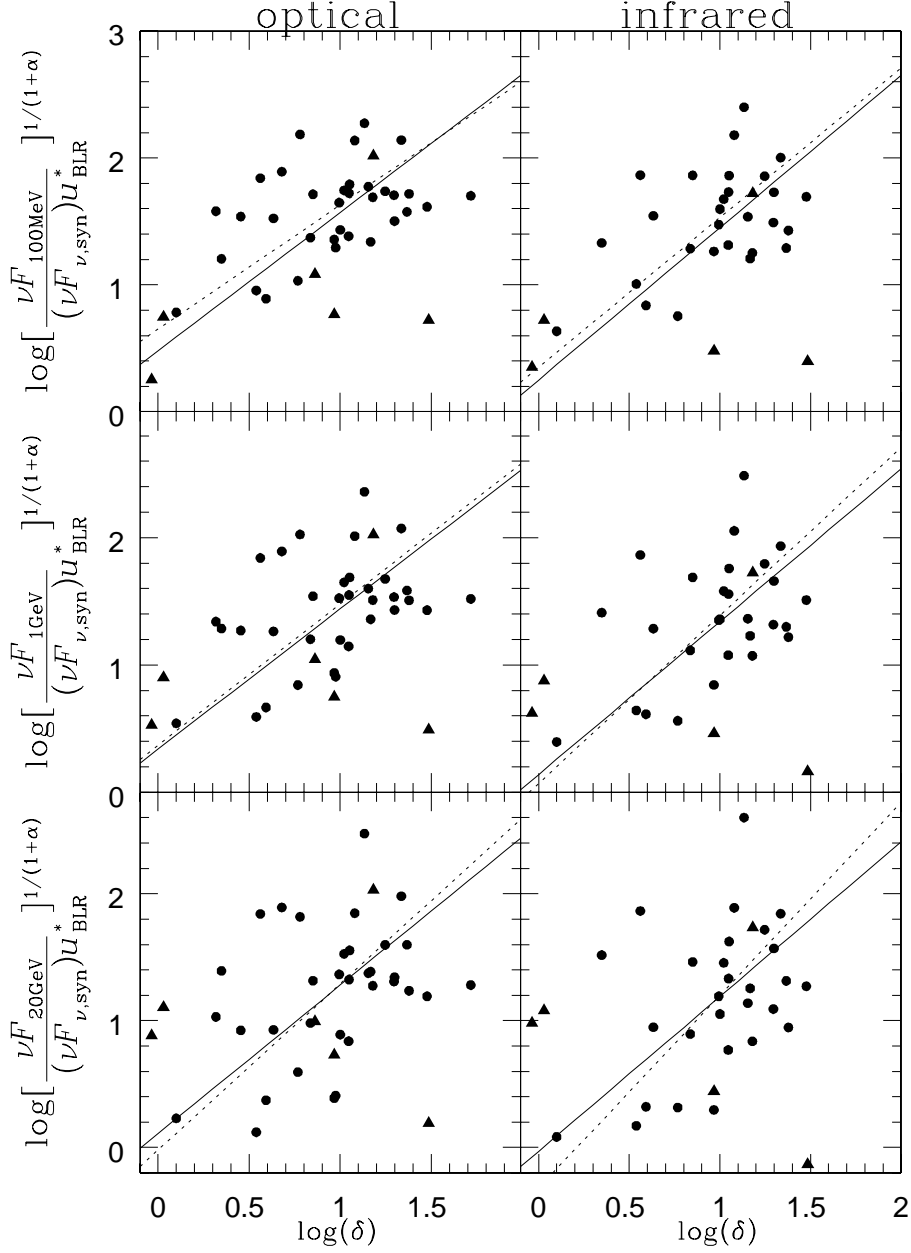


Fig. 1.— The relations of the Doppler factor δ versus the flux ratio $(\nu F_{\nu,\gamma}/\nu F_{\nu,\text{syn}}u_{\text{BLR}}^*)^{1/(1+\alpha)}$. The top, middle, and bottom panels are the cases for F_γ at 100 MeV, 1 GeV and 20 GeV, respectively. While all left panels are for F_{syn} at 5500 Å, all right panels are for F_{syn} at 2.2 μm . The filled circles represent quasars, and the filled triangles are BL Lac objects.

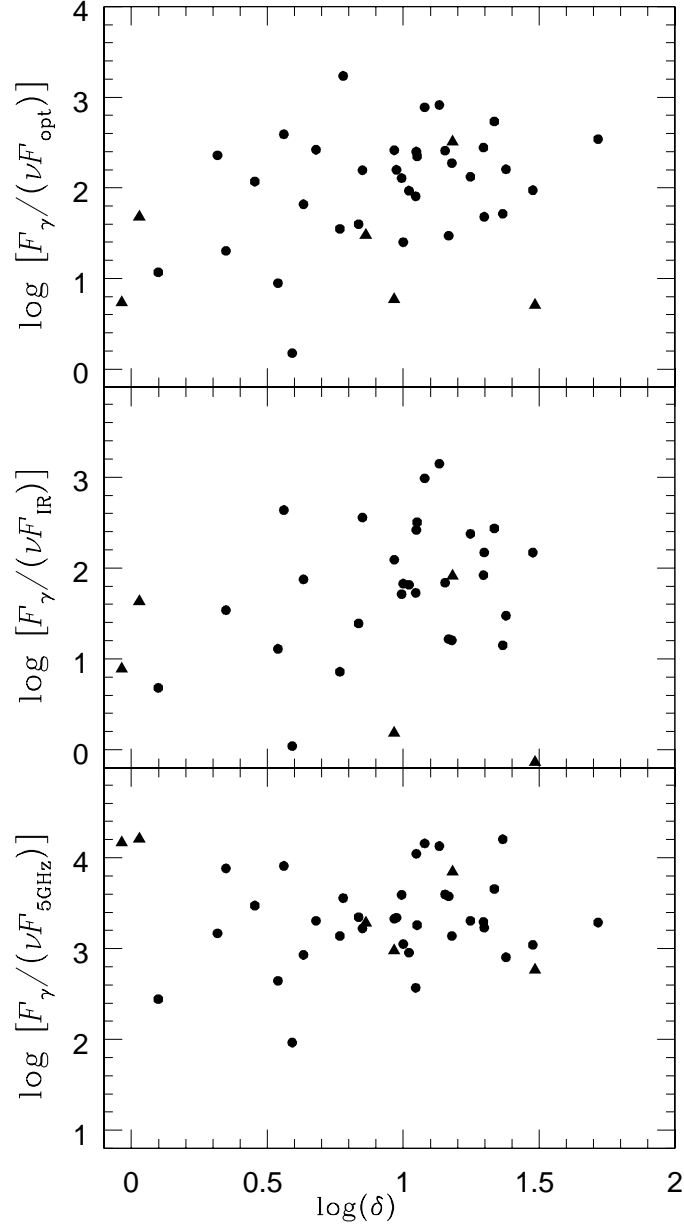


Fig. 2.— Doppler factor δ versus $F_\gamma/\nu F_{\text{opt}}$, $F_\gamma/\nu F_{\text{IR}}$, and $F_\gamma/\nu F_{5\text{GHz}}$ in top, middle, bottom panels, respectively. The symbols are the same as in Fig. 1.

Table 1. VLBI and X-ray data of the selected AGNs

Source	ID*	type	z	θ_d mas	$F_c(\nu_s)$ Jy	ν_s GHz	Ref.	F_X μ Jy	Ref.	δ
0119+041	a	Q	0.637	0.310	0.580	8.55	F00	0.12	W94	2.08
0208–512	A	BL	1.003	0.350	2.770	5.00	HJ99	0.61	C97	15.17
0234+285	a	Q	1.213	0.070	1.470	22.20	J01	0.09	C97	23.86
0235+164	A	Q	0.940	0.080	0.705	43.20	J01	0.78	C97	2.23
0336–019	A	Q	0.852	0.570	1.520	2.30	HJ99	0.10	C97	13.58
0414–189	A	Q	1.536	0.180	0.760	8.55	F00	0.19	S98	9.44
0420–014	A	Q	0.914	0.060	2.724	43.20	J01	0.44	C97	15.10
0454–234	A	Q	1.003	0.070	0.575	43.20	J01	0.09	C97	3.46
0458–020	A	Q	2.286	0.024	0.934	43.20	J01	0.10	C97	52.14
0521–365	a	Q	0.055	0.730	1.820	5.000	HJ99	2.12	C97	1.26
0537–441	A	Q	0.894	0.600	3.370	5.00	HJ99	0.81	C97	6.86
0804+499	a	Q	1.433	0.060	0.970	22.20	J01	0.17	C97	19.84
0827+243	A	Q	0.939	0.050	1.407	43.20	J01	0.34	C97	11.16
0836+710	A	Q	2.170	0.065	1.570	43.20	J01	1.60	C97	10.00
0851+202	A	BL	0.306	0.043	1.640	43.20	J01	0.97	C97	9.27
0954+658	A	BL	0.368	0.053	0.517	22.20	J01	0.17	C97	7.28
1101+384	A	BL	0.030	0.240	0.366	5.00	HJ99	33.80	C97	0.92
1127–145	a	Q	1.187	0.140	1.060	22.20	J01	0.34	C97	4.29
1156+295	A	Q	0.729	0.046	1.372	22.20	J01	0.80	C97	23.25
1219+285	A	BL	0.102	0.090	0.263	22.20	J01	0.41	C97	1.07
1222+216	A	Q	0.435	0.060	0.960	22.20	J01	0.41	C97	9.87
1226+023	A	Q	0.158	0.135	8.040	43.20	J01	12.30	C97	3.91
1243–072	A	Q	1.286	0.740	0.540	2.32	F00	0.52	S98	2.85
1253–055	A	Q	0.538	0.072	5.440	43.20	J01	1.34	C97	14.69
1334–127	A	Q	0.539	0.490	4.100	5.00	SZ98	0.33	S98	11.12
1406–076	A	Q	1.494	0.075	0.833	22.20	J01	0.18	S98	12.00
1424–418	A	Q	1.522	0.469	3.315	5.00	FF0	0.18	M05	17.67
1504–166	a	Q	0.876	0.220	0.770	8.55	F00	0.27	S98	4.78
1510–089	A	Q	0.360	0.056	1.458	43.20	J01	0.74	C97	5.85
1611+343	A	Q	1.401	0.080	1.460	43.20	J01	0.24	C97	7.08
1633+382	A	Q	1.814	0.075	1.553	22.20	J01	0.42	C97	21.64
1730–130	A	Q	0.902	0.078	3.350	43.20	J01	0.63	C97	11.26
1739+522	A	Q	1.375	0.073	0.973	22.20	J01	0.16	C97	14.25
1741–038	A	Q	1.054	0.130	5.105	22.20	J01	0.61	C97	19.72
1936–155	A	Q	1.657	0.680	0.860	2.32	F00	0.05	W94	9.26
2200+420	A	BL	0.069	0.033	4.123	43.00	L01	0.82	G93	30.52
2230+114	A	Q	1.037	0.040	2.429	43.20	J01	0.29	C97	30.02
2251+158	A	Q	0.859	0.054	2.016	43.20	J01	1.37	C97	10.49
2320–035	A	Q	1.410	0.190	0.330	8.55	F00	0.17	S98	3.64
2351+456	A	Q	1.992	0.088	1.209	43.00	L01	0.31	G93	6.01

*A is high-confidence identifications of blazars, a is lower confidence identifications of potential blazars

References. — C97: Comastri (1997); F00: Fey & Charlot (2000); FF0: Fomalont et al. (2000); G93: Ghisellini et al. (1993); HJ99: Huang, Jiang & Cao (1999); J01: Jorstad et al. (2001); L01: Lister (2001); M05: Marshall (2005); SZ98: Shen et al. (1998); S98: Siebert et al. (1998); W94:

Wilkes et al. (1994)

Table 2. Multi-band data of the selected AGNs

Source	α	F_γ	F_{opt} mJy	Ref.	F_{IR} mJy	Ref. ^a	$F_{5\text{GHz}}$ Jy	Ref. ^b	$F_{\text{H}\beta}^c$	Ref.	$\log u_{\text{BLR}}^*$ ergs cm ⁻³
0119+041	1.63	20.30	0.065	K81	...		1.10	FF0	5.800	JB91	-1.981
0208-512	0.99	134.1	0.660	D95	10.39	2MS	3.31	F98	11.65	SF97	-2.244
0234+285	1.53	31.40	0.156	D95	3.360	B01	3.40	FF0	19.66	W84	-2.388
0235+164	0.85	65.10	6.600	D95	15.48	S96	1.90	FF0	0.802	C87	-1.833
0336-019	0.84	177.6	0.450	C97	1.053	B01	3.00	FF0	12.00	JB91	-2.190
0414-189	2.25	49.50	0.165	K81	...		1.30	FF0	0.388	H78	-1.903
0420-014	1.44	64.02	0.296	D95	13.90	X98	4.40	FF0	8.347	SF97	-2.162
0454-234	2.14	14.70	0.910	D95	2.510	X98	2.00	FF0	2.051	S89	-1.992
0458-020	1.45	68.20	0.170	D95	...		3.30	FF0	0.185	B89	-1.938
0521-365	1.63	31.90	2.000	D95	19.50	F93	9.20	FF0	5.200	SF97	-1.172
0537-441	1.41	91.10	2.050	D95	13.29	X98	4.00	F98	3.818	SF97	-2.041
0804+499	1.15	15.10	0.390	D95	0.505	C99	1.20	FF0	1.935	L96	-2.112
0827+243	1.42	111.0	0.391	D95	1.497	B01	0.97	Z01	4.937	G01	-2.096
0836+710	1.62	33.40	0.980	D95	1.467	B01	2.40	FF0	13.83	L96	-2.545
0851+202	1.03	15.80	4.000	C97	61.80	G85	2.70	FF0	1.010	S89	-1.475
0954+658	1.08	18.00	0.820	C97	...		1.40	FF0	0.417	L96	-1.409
1101+384	0.57	27.10	17.80	D95	50.13	M90	0.72	Z01	4.528	M92	-0.969
1127-145	1.70	61.80	0.652	C97	2.295	B01	5.50	FF0	29.26	W95	-2.438
1156+295	0.98	163.2	5.100	D95	74.80	X98	1.80	FF0	13.46	W83	-2.151
1219+285	0.73	53.60	2.900	C97	12.85	X98	0.94	Z01	0.049	M96	-0.683
1222+216	1.28	48.10	0.390	C97	3.873	B01	1.40	FF0	30.90	S87	-2.091
1226+023	1.58	48.30	24.60	D95	134.8	X98	43.6	FF0	1720.	K00	-2.338
1243-072	1.73	44.10	0.256	K81	...		1.10	FF0	6.838	W86	-2.256
1253-055	0.96	267.3	15.10	D95	108.8	X98	13.0	FF0	5.824	SF97	-1.922
1334-127	1.62	20.20	0.185	K81	1.124	B01	4.40	FF0	5.202	S93	-1.907
1406-076	1.29	128.4	0.170	D95	0.544	2MS	1.00	FF0	16.66	W86	-2.439
1424-418	1.13	55.30	0.532	K81	1.188	2MS	3.80	FF0	2.352	SF97	-2.162
1504-166	1.00	33.20	0.197	K81	...		2.80	FF0	5.500	SF97	-2.087
1510-089	1.47	49.40	1.180	D95	23.09	X98	3.30	FF0	0.195	JB91	-1.291
1611+343	1.42	68.90	0.390	D95	0.681	B94	4.00	FF0	6.524	W95	-2.280
1633+382	1.15	107.5	0.246	D95	1.950	X98	3.20	FF0	9.965	L96	-2.434
1730-130	1.23	104.8	0.520	C97	1.457	2MS	7.00	FF0	7.000	J84	-2.132
1739+522	1.42	44.90	0.155	D95	2.314	2MS	1.10	FF0	4.186	L96	-2.209
1741-038	1.42	48.70	0.155	D95	2.074	2MS	2.40	FF0	2.109	S89	-2.014
1936-155	2.45	55.00	0.105	K81	0.886	B01	1.40	FF0	1.294	SF97	-2.105
2200+420	1.60	39.90	5.900	G93	165.0	X98	5.60	FF0	13.00	V95	-1.372
2230+114	1.45	51.60	0.470	D95	1.200	X98	4.40	FF0	14.24	SF97	-2.285
2251+158	1.21	116.1	1.420	D95	8.100	X98	16.0	FF0	47.03	W95	-2.391
2320-035	1.00	38.20	0.153	K81	0.551	B01	0.80	NED	0.258	B89	-1.814
2351+456	1.38	42.80	0.023	G93	...		1.20	FF0	3.691	L96	-2.323

^a2MS is 2MASS

^bNED is from NED website

^cthe flux of H β emission line, in unit of 10⁻¹⁵ ergs cm⁻² s⁻¹

References. — B89: Baldwin, Wampller & Gaskell (1989); B94: Bloom et al. (1994); B01: Barkhouse (2001);

C87: Cohen et al. (1987); C97: Comastri (1997); C99: Chapuis et al. (1999); D95: Dondi & Ghisellini (1995); F93: Falomo, Bersanelli, Bouchet & Tanzi (1993); F98: Fan et al. (1998); FF0: Fomalont et al. (2000); G85: Gear et al. (1985); G93: Ghisellini et al. (1993); G01: Gu, Cao & Jiang (2001); H78: Hunstead, Murdoch & Shobbrook (1978); J84: Junkkarinen (1984); JB91: Jackson & Browne (1991); K81: Küehr (1981); K00: Kaspi et al. (2000); L96: Lawrence et al. (1996); M90: Mead et al. (1990); M92: Morganti, Ulrich & Tadhunter (1992); M96: Marcha et al. (1996); S87: Stockton & Mackenty (1987); S89: Stickel, Fried & Kühr (1989); S93: Stickel, Kühr & Fried (1993); S96: Sambruna, Maraschi & Urry (1996); SF97: Scarpa & Falomo (1997); V95: Vermeulen et al. (1995); W83: Wills et al. (1983); W84: Wampler, Gaskell & Burke (1984); W86: Wilkes (1986); W95: Wills et al. (1995); X98: Xie et al. (1998); Z01: Zhang, Cheng & Fan (2001)

Table 3. Results of the correlation analysis

y	x	N	a	SD(a)	b	SD(b)	r	prob	note
$\log\left[\frac{\nu F_{100\text{MeV}}}{(\nu F_{\text{opt}})u_{\text{BLR}}^*}\right]^{1/(1+\alpha)}$	$\log(\delta)$	40	0.481	0.105	1.089	0.092	0.494	0.714D-03	
		34	0.650	0.106	0.979	0.105	0.457	0.461D-02	excluding BLO
$\log\left[\frac{\nu F_{1\text{GeV}}}{(\nu F_{\text{opt}})u_{\text{BLR}}^*}\right]^{1/(1+\alpha)}$	$\log(\delta)$	40	0.339	0.111	1.104	0.096	0.420	0.520D-02	
		34	0.367	0.134	1.113	0.127	0.432	0.785D-02	excluding BLO
$\log\left[\frac{\nu F_{20\text{GeV}}}{(\nu F_{\text{opt}})u_{\text{BLR}}^*}\right]^{1/(1+\alpha)}$	$\log(\delta)$	40	0.108	0.146	1.172	0.120	0.294	0.586D-01	
		34	-0.020	0.190	1.307	0.169	0.388	0.186D-01	excluding BLO
$\log\left[\frac{\nu F_{100\text{MeV}}}{(\nu F_{\text{IR}})u_{\text{BLR}}^*}\right]^{1/(1+\alpha)}$	$\log(\delta)$	33	0.253	0.128	1.203	0.104	0.464	0.446D-02	
		28	0.346	0.150	1.181	0.142	0.484	0.600D-02	excluding BLO
$\log\left[\frac{\nu F_{1\text{GeV}}}{(\nu F_{\text{IR}})u_{\text{BLR}}^*}\right]^{1/(1+\alpha)}$	$\log(\delta)$	33	0.137	0.144	1.202	0.119	0.375	0.255D-01	
		28	0.065	0.193	1.319	0.179	0.464	0.912D-02	excluding BLO
$\log\left[\frac{\nu F_{20\text{GeV}}}{(\nu F_{\text{IR}})u_{\text{BLR}}^*}\right]^{1/(1+\alpha)}$	$\log(\delta)$	33	-0.029	0.200	1.217	0.172	0.246	0.156D+00	
		28	-0.321	0.281	1.521	0.251	0.424	0.186D-01	excluding BLO
$\log\left[\frac{\nu F_{100\text{MeV}}}{(\nu F_{5\text{GHz}})u_{\text{BLR}}^*}\right]^{1/(1+\alpha)}$	$\log(\delta)$	40	1.222	0.093	0.980	0.039	0.164	0.301D+00	
		34	1.147	0.103	1.030	0.089	0.342	0.404D-01	excluding BLO
$\log\left[\frac{\nu F_{1\text{GeV}}}{(\nu F_{5\text{GHz}})u_{\text{BLR}}^*}\right]^{1/(1+\alpha)}$	$\log(\delta)$	40	1.050	0.136	1.027	0.081	0.071	0.657D+00	
		34	0.848	0.156	1.181	0.136	0.311	0.646D-01	excluding BLO
$\log\left[\frac{\nu F_{20\text{GeV}}}{(\nu F_{5\text{GHz}})u_{\text{BLR}}^*}\right]^{1/(1+\alpha)}$	$\log(\delta)$	40	2.753	0.232	-1.002	0.193	-0.002	0.990D+00	
		34	0.487	0.257	1.347	0.232	0.282	0.957D-01	excluding BLO

Table 4. Results of the correlation analysis

y	x	N	a	SD(a)	b	SD(b)	r	prob	note
$\log\left[\frac{F_{\gamma}}{\nu F_{\text{opt}}}\right]$	$\log(\delta)$	40	0.670	0.199	1.371	0.170	0.338	0.279D-01	
		34	0.687	0.269	1.423	0.226	0.368	0.266D-01	excluding BLO
$\log\left[\frac{F_{\gamma}}{\nu F_{\text{IR}}}\right]$	$\log(\delta)$	33	0.372	0.253	1.386	0.262	0.237	0.171D+00	
		28	0.151	0.352	1.698	0.324	0.382	0.366D-01	excluding BLO
$\log\left[\frac{F_{\gamma}}{\nu F_{5\text{GHz}}}\right]$	$\log(\delta)$	40	4.286	0.142	-1.018	0.087	-0.039	0.808D+00	
		34	2.211	0.179	1.157	0.152	0.249	0.144D+00	excluding BLO